Research Article

Straightforward and Cost-Effective Production of RADA-16I Peptide in *Escherichia coli*

Mohamad Hassan Fouani [1], Maryam Nikkhah [2,*], Javad Mowla [3]

[1] PhD Candidate, Department of Nanobiotechnology, Faculty of Biological Sciences, Tarbiat Modares University, Tehran, Iran

[2] Associate Professor, Department of Nanobiotechnology, Tarbiat Modares University, Tehran, Iran

[3] Professor, Faculty of Biological Sciences, Tarbiat Modares University Tehran, Iran

[*] **Corresponding author:** Maryam Nikkhah, Associate Professor, Department of Nanobiotechnology, Tarbiat Modares University, Tehran, Iran. E-mail: m_nikkhah@modares.ac.ir

Abstract

Background: RADA16I represents one of promising hydrogel forming peptides. Several implementations of RADA16I hydrogels have proven successful in the field of regenerative medicine and tissue engineering. However, RADA16I peptides used in various studies utilize synthetic peptides and so far, only two research articles have been published on RADA16I peptide recombinant production. Moreover, previous studies utilized non- or less routine expression and purification methods to produce RADA16I peptide recombinantly.

Objectives: The main goal was to produce the self-assembling peptide, RADA16I, in *Escherichia coli* by exploiting routine and widely used vectors and purification methods, in shake flask.

Material and Methods: RADA16I coding sequence was inserted in pET31b+, and the construct was transformed into E. coli. Purified fusion constructs were purified using Nickel Sepharose. RADA16I unimers were released using CNBr cleavage. CD and FTIR spectroscopy were used to study recombinant RADA16I's confirmation. TEM was used to confirm fibril formation of recombinant RADA16I. Furthermore, MTT assay was implemented to assess cytocompatibility of recombinant RADA16I.

Results: The biochemical, biophysical and structural analysis proved the ability of the recombinant RADA16I to form self-assembling peptide nanofibers. Furthermore, the nanofibers exhibited no cytotoxicity and retained their cell adhesive activity.

Conclusions: We successfully produced RADA16I in acceptable levels and established a basis for future investigation for the production of RADA16I under fermentation conditions.

Keywords: Fusion Protein; Hydrogel; Nanofibers; RADA16I; Self-Assembling Peptide

1. Background

Among many challenges in tissue engineering is the development of biomaterials that support cellular functions, such as cell adhesion, growth and differentiation (1). Small biological molecules capable of self-assembly and degradation over time into predictable metabolites represent ideal candidates for scaffolds to regenerate tissues and organs. For instance, peptide base self-assembling peptide nanofibers maintain functionality within a desired period of time, as well as the byproducts resulting from their degradation introduce no toxic constituents to their surrounding environment(2).

RADA-16I peptide the well-studied self-assembling peptide nanofiber (SAPN) was first introduced by S.

Zhang (3) who has inspired the design of RADA16I from the set of tandem repeats, namely EAK16 (AEAEAKAKAEAEAKAK), present in the yeast Zuotin protein (4). In RADA-16I peptide, with the (RADARADARADARADARADA) sequence, the four amino acid RADA motif, hence annotation 16; whereas the I is used to discriminate it from RADA-16II which has the following sequence (RARADADARARADADA) (5). RADA-16I exhibits an intrinsic capability to form hydrogels in the presence of monovalent salts or under physiological conditions due to the ionic interactions and the tendency of the backbone to adopt β-sheet structure (4, 6). There is extensive literature regarding the

biophysical and biochemical properties of RADA-16I as well as on the various conditions at which RADA-16I forms hydrogel (7-13).

Several biological implementations of RADA-16I based hydrogels have proven successful. For example, S. Zhang has proven the ability of RADA-16I to support the attachment and differentiation of a broad range of cell types among which are neuronal stem cells, hepatic stem cells and cardiac myocytes (3, 4, 14-16). S. Zhang *etal* further demonstrated the ability of RADA-16I to promote angiogenesis (17). Other researchers have elaborated RADA-16I ability to repair brain, spinal and neuronal tissue injuries (18-20). In another study S. Zhang *etal* used RADA-16I hydrogels for the sake of cartilage tissue repair (21). Moreover, there is clear evidence on RADA-16I's capability to stop bleeding (complete hemostasis) immediately when directly treating brain, spinal cord, femoral artery, liver, or skin wounds(18).
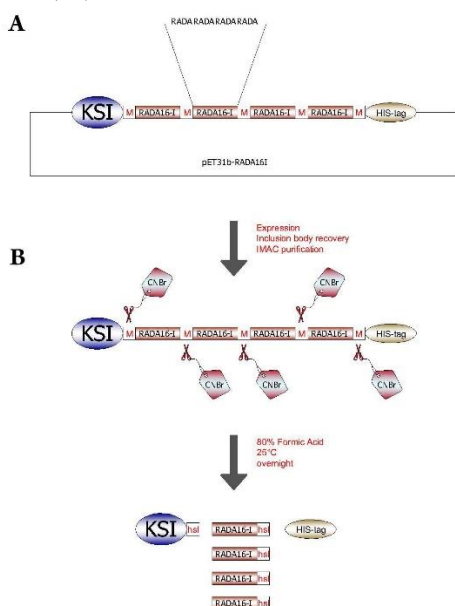
Figure 1. Cloning and Expression stratagies for RADA16I peptide repeats. a) Four RADA16I repeats were inserted between KSI and HIS-tag. Methionine spacers were located between the repeats, as well as between the repeats and both KSI and HIS-tag. b) Following protein expression, inclusion body recovery and IMAC purification the KSI-[RADA16I]4-HIS-tag is treated with CNBr to generate a mixture of KSI, RADA16I unimers and HIS-tag.

2. Objectives

Here we describe a novel straight forward method for the recombinant production of RADA-16I based on the method initially described by T. Walsh(22). Briefly, Keto Steroid Isomerease (KSI)/ RADA-16I /His-tag fusion expressed in E. coli was purified using affinity chromatography and then cleaved with Cyanogen Bromide (CNBr) to release RADA-16I peptides (**Fig. 1**); in the end fibril formation was confirmed. Furthermore, fibrils formed proved to be non-cytotoxic, promote cell proliferation and exhibited cell adhesivity.

3. Materials and Methods

3.1. Bacterial Strains, Plasmid, and Culture Media
Escherichia coli Stbl3 strain was used for routine cloning, whilst *E. coli*
BL21 (DE3) pLysS strain was used for the expression of the pET31b+/ RADA-16I construct.
E. coli strains were grown in Super Optimal broth with Catabolite repression
(SOC) medium, containing 2% w.v^{-1} Tryptone, 0.5% w.v^{-1} Yeast extract, 10 mM NaCl,
2.5 mM KCl, 10 mM MgCl$_2$, 10 mM MgSO$_4$, and 20 mM Glucose. Ampicillin was added to the media at a final concentration of 100 µg mL^{-1}. Competent *E. coli* strains were prepared and transformed according to the protocol described by Inoue et al (23).

3.2. Protein Expression and Purification
In order to express the recombinant construct, pre-cultures (10 mL) from single colonies were incubated with shaking at 18°C for 18 hours. Subsequently, 25 µL of the pre-culture were added to 250 mL SOC medium in a 1 L conical flask and grown with shaking at 18°C until it reached OD$_{600}$~0.8 (18 h). Isopropyl-b-D-Thiogalactopyranoside (IPTG) was added to final concentration 0.8 mM to induce protein expression. The bacteria were kept shaking at 250 rpm in an orbital incubator at 18° C for 6 hours. Afterwards, cells were harvested by centrifugation at 1792 *g* using a fixed angle rotor. In order to extract IBs, 10 mL Lysis Buffer (20 mM sodium phosphate, 500 mM NaCl, 8 M Urea) was added to the bacterial pellet obtained from 250 mL culture, and subsequently sonicated on ice to lyse the cells thoroughly. Lysates were then centrifuged (18928 g, 4°C) and aliquots of the supernatant were stored at -20°C for subsequent analysis.
A 5 ml HisTrap chelating column (GE Healthcare UK Ltd.) was used to purify KSI fusion proteins according to the manufacturer's instructions. Before loading the supernatant, 0.45 µm syringe filter was used to remove any insoluble materials.

3.3. Cleavage of the KSI/ RADA-16I /His Protein by Cyanogen Bromide
Purified KSI/ RADA-16I /His were dialyzed against distilled water over night, and subsequently freeze-dried. KSI/ RADA-16I /His dried sample (10-20 mg.mL^{-1}) was dissolved in 70% formic acid and then Cyanogen Bromide (CNBr) added to the protein sample at a 200-molar excess to methionine residues in a 2 mL volume. The tube was capped and incubated for 18-20 h at room temperature in the dark. Subsequently, the CNBr cleaved KSI/ RADA-16I /His mixture was dried by rotary evaporation. The gelatinous material formed was resuspended in 20 mM KH$_2$PO$_4$, 100 mM NaCl, and the pH adjusted to 7.4 with 1 M NaHCO$_3$. This mixture was stirred overnight under N$_2$ at room temperature in darkness. Afterwards, the suspension

was centrifuged at 18928 *g* for 45 min at 4°C and the supernatant was collected.

3.4. RP-HPLC and Mass Spectrometry

RP-HPLC was performed using an analytical Zorbax SB-C18C18 column (15 cm, 3.5 μm) from Agilent, with a linear gradient of acetonitrile from 5% to 55% in a 0.1% Formic acid solution. The flow rate was 0.3 mL.min^{-1} for 20 min. Purified peptides were quantified via absorbance measurement at 215 nm Peak fractions obtained from RP-HPLC were freeze-dried prior to analysis by mass spectrometry. Positive Electron Spray Ionization (ESI) was carried out on Agilent G6410 Triple Quadrapole Mass spectrometer.

3.5. Circular Dichroism (CD)

Jasco Spectro-polarimeter J-715 (Tokyo, Japan) was used to perform Circular dichroism measurements. Far-UV CD spectra were recorded from 190 to 260 nm with the temperature of the cell holder controlled at 25 °C. Data obtained were smoothed with J-715 software, followed by processing and deconvoluting by ORIGIN software.

3.6. Fourier Transform Infrared Spectroscopy (FTIR)

FTIR was used to further assign the secondary structure of dissolved recombinant RADA-16I. Two RADA-16I concentrations (2.5 and 0.5 mg.mL^{-1}) were prepared. From each sample 100 μL were deposited on Potassium Bromide (KBr) discs. The FTIR spectrum corresponding to the discs was taken at a wavenumber resolution of 4 cm^{-1} using Tensor 27 FT-IR spectrometer. Measurements were recorded within 500-4000 cm^{-1}, where the amide I band is expected to appear.

3.7. Transmission Electron Microscopy

Thirty microliters of RADA-16I samples (2.5 and 0.5 mg.mL^{-1} samples of RADA-16I) were applied to a 300-mesh formvar/carbon-coated nickel grid and after 2 min, stained with 3% uranyl acetate for 2 minutes, rinsed, and air-dried. Images were taken using Zeiss-EM10C-80 KV transmission electron microscope (Oberkochen, Germany).

3.8. Assessment of Purified RADA-16I Peptide Cell Toxicity

MCF-7 cells were cultured in a 96-well flask with 5x10^3 cells in each well. The next day, MCF-7 cells were exposed to purified recombinant RADA-16I peptide, at a final concentration 0.5% w.v^{-1} and 1% w.v^{-1}, for 24 hours; control groups were treated similarly with recombinant RADA-16I free media. Later on, the medium was aspirated and a medium was added with a final concentration of MTT equal to 5 mg.mL^{-1}. The cells were incubated for 4 h at 37° C. Then the medium was aspirated carefully without disturbing the formed formazan crystals, which were then dissolved using 100 μL of DMSO (dimethyl sulfoxide). After complete

solubilization of formazan crystals, absorbance was recorded at 570 nm.

3.9. Evaluation of Purified RADA-16I Peptide Cell Adhesive Activity

For coating glass cover slips, 50 μL of purified peptides (100, 250, 500, and 1000 μM) diluted in 1X phosphate buffer saline (PBS) were spread on the top of the glass cover slips, which in turn were embedded at the bottom of 6-well plates and left to dry at 37 °C. After complete dryness, 3x10^3 MCF-7 cells in Dulbecco's Modified Eagle's medium were seeded on the glass cover slips. After Incubation for 48 h, cover slips were observed under light microscope.

4. Results

4.1. Expression and of Purification of Recombinant RADA-16I

The integrity of the pET-31 KSI/ RADA-16I /His construct was confirmed by sequencing (Data not shown). The expressed recombinant protein present in the pellet of the bacterial lysate, i.e. inclusion bodies, was analyzed using SDS-PAGE (**Fig. 2A**). The molecular weight of the fusion protein KSI/ RADA-16I /His (21.28 kDa) was confirmed through comparison with protein ladder (**Fig. 2A**) were it ranged from 20 kDa to 25 kDa; both the crude lysate (**Fig. 2A**) and purified (**Fig. 2B**) fusion protein KSI/ RADA-16I /His proved to match the expected molecular weight.

4.2. CNBr Cleavage, Purification and Confirmation of Recombinant RADA-16I

Purified KSI/ RADA-16I /His fusion protein were dialyzed against ddH2O and subsequently freeze-dried. Dried samples were digested with CNBr which specifically cleaved the fusion protein at the Methionine junction to release insoluble KSI, the His6 tag, and recombinant RADA-16I. The digestion reaction was analyzed with SDS-PAGE (**Fig. 2C**). It is clear from the gel electrograph that complete digestion of the fusion protein took place since we can observe a band located between 11 kDa to 17 kDa, the molecular weight corresponding to KSI (14 kDa).

Following the incubation with CNBr, the reaction was dried using rotary evaporation in order to remove formic acid. A gelatinous material was observed at the bottom of the reaction tubes. The gelatinous material was then resuspended in 20 mM KH2PO4, 100 mM NaCl buffer. The solution was extensively centrifuged, and the resulting supernatant were RADA-16I is expected to be was subjected to RP-HPLC. The RP-HPLC purified peptides were freeze-dried and then solubilized in 65% formic acid and used for electrospray ionization mass spectrometry for further characterization. The determined molecular weight of recombinant RADA16I obtained from CNBr cleavage is 1774.2 Da, as shown in (**Fig. 2D**).
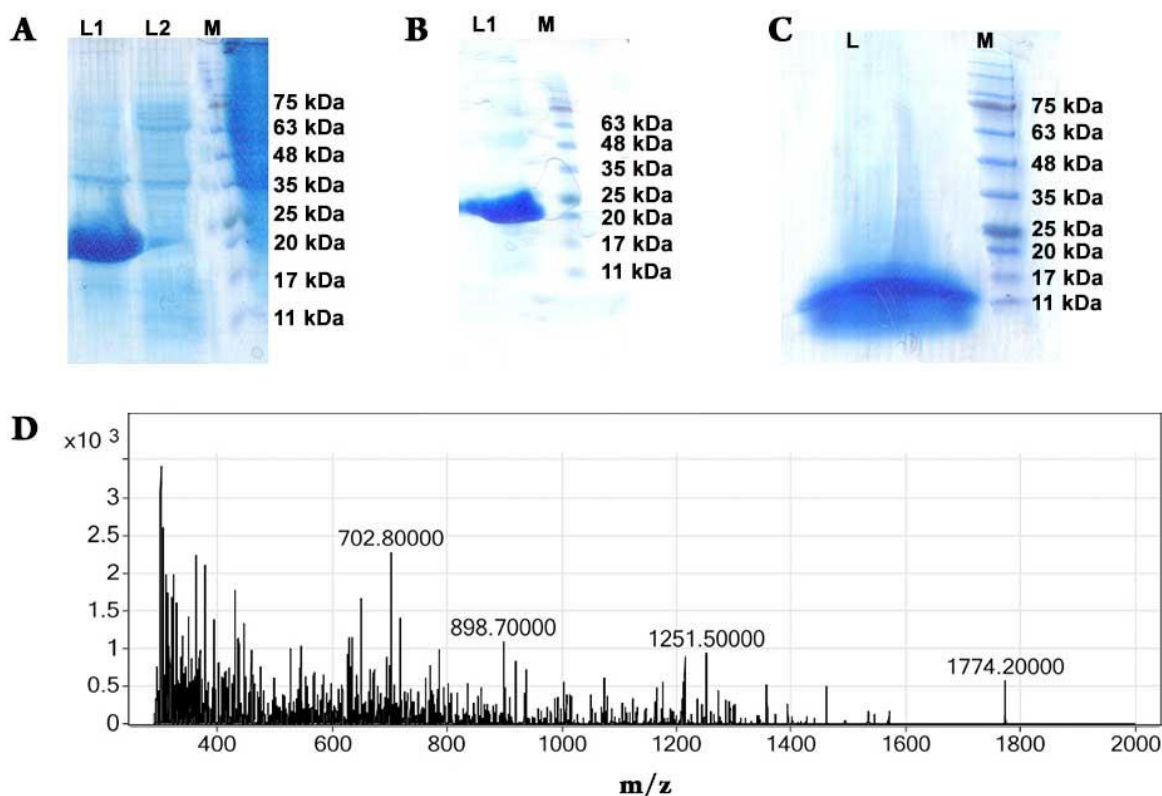
Figure 2. Expression, purification and CNBr digestion of KSI-[RADA16I]4-HIS-tag constructs. A) SDS–PAGE analysis of 0.8 mM IPTG-induced expression of KSI fusion constructs carrying RADA16I peptide repeats. L1, pelet of bacterial lysate; L2, supernatant of bacterial lysate; M, molecular lader. B) SDS–PAGE analysis of KSI-[RADA16I]4-HIS-tag constructs. L1, purified KSI-[RADA16I]4-HIS-tag constructs M, molecular lader. C) SDS–PAGE analysis of the CNBr digested KSI-[RADA16I]4-HIS-tag fusion protein. L, digestion mixture; M, molecular ladder. D) Mass spectrum of RADA16I recovered by RP-HPLC following CNBr cleavage of purified KSI-[RADA16I]4-HIS-tag constructs. The monoisotopic mass of 1772.85 Da corresponds to the theoretical mass of RADA16I, 1774.20 Da

4.3. Evaluation of β-Sheet Formation by RADA16I

One of the well-recognized characteristics of RADA16I peptide is its ability to form β-sheet structures. There are several techniques to evaluate this criterion. We examined the secondary structure of recombinant RADA16I by CD and FTIR. Purified recombinant RADA16I were diluted in distilled water to a final concentration of 300 mM and it exhibited a sharp minimum ellipticity at ~205 nm, slight minimum ellipticity at ~216 nm, and a maximum ellipticity at ~192 nm (**Fig. 3A**); which is consistent with previous reports(3, 10). J-715 software estimated the β-sheet content of the RADA16I peptide to be ~82.9%.

FTIR was also used to study the secondary structure of recombinant RADA16I. FTIR analysis of RADA16I further supported CD data showing that a strong peak was observed at 1638.41 which confirmed the antiparallel β-sheet configuration of RADA16I (**Fig. 3B**).

4.4. Fibril Observation by Transmission Electron Microscopy

After confirming the adoption of β-sheet conformation by the recombinant RADA16I peptides, observation of fibril formation by transmission electron microscope was the next validation step. At low concentrations 300 mM, recombinant RADA16I exhibited fibrils with ~8nm diameter (Data not shown), whilst at higher concentrations, recombinant RADA16I peptide fibrils were noted to be interconnecting. It was also evident that fibrils were extended and twisted, as well as forming a mesh-like appearance; neighboring fibrils can be seen as fibrillar bundles and entanglements (**Fig. 4A**).
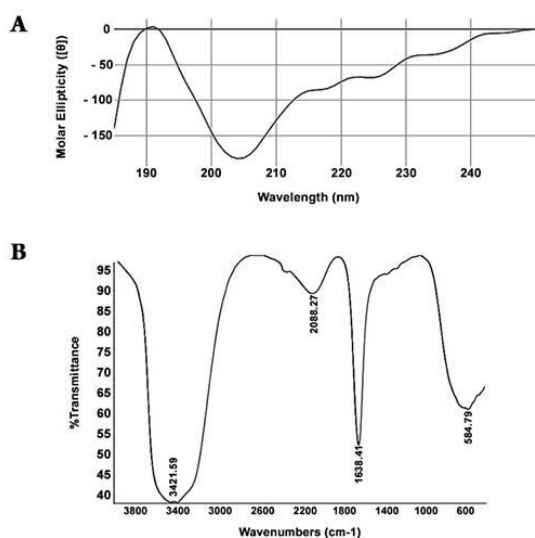
Figure 3. Secondary structure analysis of RADA16I. A) CD spectrum of RADA16I; B) Fourier transform IR spectra of amide I (1700-1600 cm^{-1}) and amide II (1600-1500 cm^{-1}) bands of RADA16I.

## 4.5. Assessing Recombinant RADA16I's Cytotoxicity and Cell Adhesion Activity

MTT assay was implemented to assess cell viability of cells exposed to recombinant RADA16I. In this regard, MCF-7 cells were exposed to recombinant RADA16I at final concentration 0.5% and 1% w/v. When compared to control samples, MCF-7 cells exposed to recombinant RADA16I at final concentration 0.5% exhibited a slight decrease in cell viability 91.85 %, whereas MCF-7 cells exposed to recombinant RADA16I at final concentration 1% exhibited an increase in cell viability 127.1 % (**Fig. 4B**).

The assessment of cell adhesive activity of recombinant RADA16I followed. To this aim, glass cover slips were coated with RADA16I, and next MCF-7 cells were seeded on these glass cover slips. FBS free DMEM was used to avoid any possible serum effects. After 48 h, applying inverted microscopy, our observations show that MCF-7 cells attached to recombinant RADA16I coated cover slips whilst no cells were observed on the surface of cover slips treated with PBS only (**Fig. 4C**).

5. Discussion

RADA16I forms nanofiber matrices which have shown great promise for tissue engineering. RADA16I is currently produced using chemical synthesis and commercially available as PuraMatrix (BD, Franklin Lakes, NJ, USA). Besides the fact that it is an expensive process in which cost increases with peptide length, F. Albericio describes the process of synthesizing and purifying RADA-16 as a "Tough" one(24). In contrast, although there are significant challenges for the production and efficient purification of short self-assembling peptides, recombinant production of RADA-16I in a bacterial host offers a potentially more

economical solution owing to its ease of use, robustness and low costs.
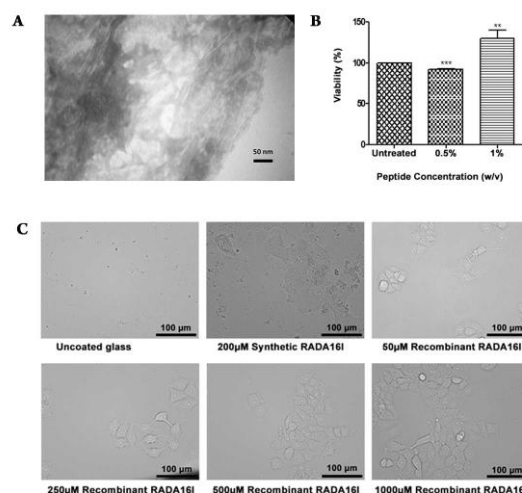
Figure 4. A) Transmission electron microscopy (TEM) image of RADA16I fibrils formed at a final peptide concentration of 2.5 mg.L-1. B) Evaluation of cell cytotoxicity of purified RADA16I fibrils. Blank, cells not treated with RADA16I; green, cells treated with 0.5% RADA16I; violet, cells treated with 1% RADA16I. C) Evaluation of cell adhesivity of purified RADA16I fibrils. i, uncoated glass cover slips; ii, glass cover slips coated with 200μM synthetic RADA16I; iii, glass cover slips coated with 50μM recombinant RADA16I; iv, glass cover slips coated with 250μM recombinant RADA16I; v, glass cover slips coated with 500μM recombinant RADA16I; vi, glass cover slips coated with 1000μM recombinant RADA16I.

For various reasons *E. coli* represents one of the attractive choices for heterologous protein production. For instance, the genetic characteristics of E. coli are well-established and has the ability to grow rapidly to high cell density using low cost media. Frequently, the recombinant protein production in E. coli is associated with the formation of intracellular protein aggregates in the form of inclusion bodies. For most protein production systems this is undesirable since recovery of functional protein from inclusion bodies involves complex refolding. However, for peptides production this is not an obstacle and recovery from inclusion bodies represents the basis of a method introduced by Walsh et al.; in this method tandem repeats of the peptide coding region are fused to KSI, the HIS-tag for purification and intervening Met residues for consequent CNBr cleavage (**Fig. 1**) (22). In this study, the goal was the enhancement of the production of RADA-16I peptide as a unimers, the introduction of a rapid and simple purification strategy and finally the characterization and cytotoxicity determination of the recombinant RADA-16I. To the best of our knowledge, so far two research articles have been published regarding the recombinant production of RADA-16I. However, when compared to our strategy, both attempts implemented novel (25) or less routine (26)

methods. For instance, Reed et al. (25) implemented pDR1 plasmid as well as Ralstonia eutropha for the RADA-16I peptide recombinant production. Under fermentation conditions, Reed et al. yield of production of fusion protein was 433 mg.L^{-1} and were able to purify 10.1 mg.L^{-1} of recombinant RADA-16I. Whereas in our case, the yield of production of fusion protein was ~95 mg.L^{-1} and were able to purify 7.8 mg.L^{-1} of RADA-16I (**Table 1**). Eiry Kobatake et al. did not report the final fusion protein or purified peptide yield in their study(26).

Table 1. Reported levels of production and purification of RADA peptide by recombinant approaches

Host	Fusion protein yield (mg/L)	Theoretical peptide yield (mg/L)	Peptide purified (mg/L)	Efficiency of peptide Purification (%)	Reference
Ralstonia eutropha	433	116	10.1	8.7	(25)
Escherichia coli	95	33.86	7.8	23.03	This work

Circular dichroism analysis indicated that a minimum is located at ~205 nm and a maximum ellipticity at ~192 nm, characteristic of random coil. The shoulder around ~216 nm corresponds to β-sheet (**Fig. 3A**). This observation could be attributed to the fact that at this concentration of purified recombinant peptide RADA-16I monomers with random coil confirmation along with fibrils with β-sheet confirmation are present concomitantly in the aqueous solution(9). However, J-715 software estimated that the β-sheet content is 85%. In the amide I, fibrils exhibit two bands; a low frequency, high intensity band around 1620–1630 cm−1 and a high frequency, low intensity band located around 1685–1695 cm^{-1}, which correspond to anti-parallel β-sheet The concurrent appearance of these two bands correspond to anti-parallel β-sheet whilst the presence of only the low frequency band around 1630–1640 cm^{-1} confers to the parallel counterpart. Hence, FTIR analysis indicated the existence of parallel β-sheet conformation (**Fig. 3B**) since it only exhibited a single band 1638.41 cm^{-1} in the amide I region (27, 28). TEM observations (**Fig. 4A**) further confirmed that recombinant RADA-16I formed fibrils with dimensions similar to what has been reported by (26).

RADA-16I is known to exhibit two criteria useful for tissue engineering and regenerative medicine, namely cytocompatibility and cell adhesivity. Recombinant RADA-16I proved to be non-cytotoxic to MCF-7 cells grown up in contact with recombinant RADA-16I for 24 hrs. Furthermore, similar to previous reports (26) recombinant RADA-16I aided the attachment of MCF-7 cells to glass cover slips (**Fig. 4B, 4C**).

6. Conclusions

We have demonstrated that RADA16I can be expressed recombinantly in E. coli using pET31b+ plasmid. Efficient purification was achieved using Nickel Sepharose, and CNBr cleavage subsequently was used to release RADA16I unimers. Under shake flask conditions, 10.1 mg.L^{-1} was the final yield of the recombinant RADA16I. Under the experimental conditions we have set, the simple culture medium SOC proved to be more suitable for the recombinant production of RADA16I peptide in comparison to the complex autoinduction medium. Spectroscopic and microscopic analysis proved that recombinant RADA16I exhibited properties similar to the previously reported recombinant and synthetic RADA16I peptide. RADA16I self-assembled into fibrils, and cytotoxicity studies indicated that recombinant RADA16I was non-cytotoxic towards MCF-7 cells. This study establishes that recombinant RADA16I peptide can be produced in a feasible manner using routine expression and purifications methods.

Conflict of Interest

There is no conflict of interest with this study.

References

1. Langer R, Vacanti JP. Tissue engineering. *Science*. 1993;**260**(5110):920-926. doi: 10.1126/science.8493529 pmid: 8493529
2. Stupp SI, Zha RH, Palmer LC, Cui H, Bitton R. Self-assembly of biomolecular soft matter. *Faraday Discuss*. 2013;**166**:9-30. doi: 10.1039/c3fd00120b pmid: 24611266
3. Zhang S, Holmes TC, DiPersio CM, Hynes RO, Su X, Rich A. Self-complementary oligopeptide matrices support mammalian cell attachment. *Biomaterials*. 1995;**16**(18):1385-1393. doi: 10.1016/0142-9612(95)96874-Y pmid: 8590765
4. Zhang S, Lockshin C, Cook R, Rich A. Unusually stable beta-sheet formation in an ionic self-complementary oligopeptide. *Biopolymers*. 1994;**34**(5):663-672. doi: 10.1002/bip.360340508 pmid: 8003624
5. Zhang S, Gelain F, Zhao X. Designer self-assembling peptide nanofiber scaffolds for 3D tissue cell cultures. *Semin Cancer Biol*. 2005;**15**(5):413-420. doi: 10.1016/j.semcancer.2005.05.007 pmid: 16061392
6. Zhang S, Holmes T, Lockshin C, Rich A. Spontaneous assembly of a self-complementary oligopeptide to form a stable macroscopic membrane. *Proc Natl Acad Sci U S A*. 1993;**90**(8):3334-3338. doi: 10.1073/pnas.90.8.3334 pmid: 7682699
7. Aramvash A, Seyedkarimi MS. All-atom molecular dynamics study of four RADA 16-I peptides: the effects of salts on cluster formation. *J Cluster Sci*. 2015;**26**(2):631-643. doi: 10.1007/s10876-014-0836-8
8. Yokoi H, Kinoshita T, Zhang S. Dynamic reassembly of peptide RADA16 nanofiber scaffold. *Proc Natl Acad Sci*

U   S   A.   2005;**102**(24):8414-8419.   doi: 10.1073/pnas.0407843102 pmid: 15939888

9.   Arosio P, Owczarz M, Wu H, Butte A, Morbidelli M. End-to-end self-assembly of RADA 16-I nanofibrils in aqueous solutions. *Biophys J.* 2012;**102**(7):1617-1626. doi: 10.1016/j.bpj.2012.03.012 pmid: 22500762

10.   Zhang H, Luo H, Zhao X. Mechanistic study of self-assembling peptide rada16-i in formation of nanofibers and   hydrogels.   *J Nanotechnol Eng Med.* 2010;**1**(1):011007. doi: 10.1115/1.4000301

11.   Cormier AR, Pang X, Zimmerman MI, Zhou HX, Paravastu AK. Molecular structure of RADA16-I designer self-assembling peptide nanofibers. *ACS Nano.* 2013;**7**(9):7562-7572. doi: 10.1021/nn401562f pmid: 23977885

12.   Nagarkar RP, Schneider JP. Synthesis and primary characterization of self-assembled peptide-based hydrogels. *Methods Mol Biol.* 2008;**474**:61-77. doi: 10.1007/978-1-59745-480-3_5 pmid: 19031061

13.   Ye Z, Zhang H, Luo H, Wang S, Zhou Q, Du X, et al. Temperature and pH effects on biophysical and morphological properties of self-assembling peptide RADA16-I. *J Pept Sci.* 2008;**14**(2):152-162. doi: 10.1002/psc.988 pmid: 18196533

14.   Holmes TC, de Lacalle S, Su X, Liu G, Rich A, Zhang S. Extensive neurite outgrowth and active synapse formation on self-assembling peptide scaffolds. *Proc Natl Acad Sci U S A.* 2000;**97**(12):6728-6733. doi: 10.1073/pnas.97.12.6728 pmid: 10841570

15.   Semino CE, Merok JR, Crane GG, Panagiotakos G, Zhang S. Functional differentiation of hepatocyte-like spheroid structures from putative liver progenitor cells in three-dimensional peptide scaffolds. *Differentiation.* 2003;**71**(4-5):262-270.   doi: 10.1046/j.1432-0436.2003.7104503.x pmid: 12823227

16.   Semino CE, Kasahara J, Hayashi Y, Zhang S. Entrapment of migrating hippocampal neural cells in three-dimensional peptide nanofiber scaffold. *Tissue Eng.*   2004;**10**(3-4):643-655.   doi: 10.1089/107632704323061997 pmid: 15165480

17.   Narmoneva DA, Oni O, Sieminski AL, Zhang S, Gertler JP, Kamm RD, et al. Self-assembling short oligopeptides and the promotion of angiogenesis. *Biomaterials.* 2005;**26**(23):4837-4846.   doi: 10.1016/j.biomaterials.2005.01.005 pmid: 15763263

18.   Ellis-Behnke RG, Liang YX, Tay DK, Kau PW, Schneider GE, Zhang S, et al. Nano hemostat solution: immediate hemostasis at the nanoscale. *Nanomedicine.*

2006;**2**(4):207-215. doi: 10.1016/j.nano.2006.08.001 pmid: 17292144

19.   Guo J, Su H, Zeng Y, Liang YX, Wong WM, Ellis-Behnke RG, et al. Reknitting the injured spinal cord by self-assembling   peptide   nanofiber   scaffold. *Nanomedicine.*   2007;**3**(4):311-321.   doi: 10.1016/j.nano.2007.09.003 pmid: 17964861

20.   Guo J, Leung KK, Su H, Yuan Q, Wang L, Chu TH, et al. Self-assembling peptide nanofiber scaffold promotes the reconstruction of acutely injured brain. *Nanomedicine.*   2009;**5**(3):345-351.   doi: 10.1016/j.nano.2008.12.001 pmid: 19268273

21.   Kisiday J, Jin M, Kurz B, Hung H, Semino C, Zhang S, et al. Self-assembling peptide hydrogel fosters chondrocyte extracellular matrix production and cell division: implications for cartilage tissue repair. *Proc Natl Acad Sci U S A.* 2002;**99**(15):9996-10001. doi: 10.1073/pnas.142309999 pmid: 12119393

22.   Kuliopulos A, Walsh CT. Production, purification, and cleavage of tandem repeats of recombinant peptides. *J Am Chem Soc.* 1994;**116**(11):4599-4607.   doi: 10.1021/ja00090a008

23.   Inoue H, Nojima H, Okayama H. High efficiency transformation of Escherichia coli with plasmids. *Gene.* 1990;**96**(1):23-28. pmid: 2265755

24.   Paradís-Bas M, Tulla-Puche J, Zompra AA, Albericio F. RADA-16: A Tough Peptide–Strategies for Synthesis and   Purification.   *Eur   J   Organ   Chem.* 2013;**2013**(26):5871-5878.   doi: 10.1002/ejoc.201300612

25.   Reed DC, Barnard GC, Anderson EB, Klein LT, Gerngross TU. Production and purification of self-assembling peptides in Ralstonia eutropha. *Protein Expr Purif.*   2006;**46**(2):179-188.   doi: 10.1016/j.pep.2005.08.023 pmid: 16249097

26.   Mie M, Oomuro M, Kobatake E. Hydrogel scaffolds composed of genetically synthesized self-assembling peptides for three-dimensional cell culture. *Polymer J.* 2013;**45**(5):504. doi: 10.1038/pj.2012.216

27.   Nevskaya NA, Chirgadze YN. Infrared spectra and resonance interactions of amide-I and II vibration of alpha-helix. *Biopolymers.* 1976;**15**(4):637-648. doi: 10.1002/bip.1976.360150404 pmid: 1252599

28.   Sarroukh R, Goormaghtigh E, Ruysschaert JM, Raussens V. ATR-FTIR: a "rejuvenated" tool to investigate amyloid proteins. *Biochim Biophys Acta.* 2013;**1828**(10):2328-2338.   doi: 10.1016/j.bbamem.2013.04.012 pmid: 23746423